Powder Technology 249 (2013) 38–42

Contents lists available at ScienceDirect

Powder Technology

journal homepage: www.elsevier.com/locate/powtec

Construction of an interpenetrated MOF-5 with high mesoporosity for hydrogen storage at low pressure

Yafei Feng, Heng Jiang, Meng Chen, Yuren Wang *

Key Laboratory of Microgravity Science, Institute of Mechanics, Chinese Academy of Sciences, Beijing 100190, People's Republic of China

ARTICLE INFO

Article history:
Received 17 April 2013
Received in revised form 22 July 2013
Accepted 27 July 2013
Available online 3 August 2013

Keywords:
Metal-organic frameworks
Hydrogen storage
Interpenetrated MOF-5
Mesopore

ABSTRACT

An interpenetrated MOF-5 with high mesoporosity was synthesized via solvothermal method. The porous texture was confirmed by X-ray diffraction (XRD), scanning electron microscope (SEM), transmission electron microscope (TEM), and N_2 adsorption/desorption analysis. And the thermal stability and hydrogen storage at low pressure of the samples were studied. The results showed that the temperature of thermal decomposition for as-prepared MOF-5 increased and more interestingly the hydrogen uptake at 77 K and low pressure could be improved. The enhancement of hydrogen uptake was considered to be originated from successful construction of interpenetrated structure and intercrystalline mesopore.

1. Introduction

With the increasing demand for alternative fuel, hydrogen has been considered as one of the best candidates because of its abundance, non-pollution and high power density. The main issues of using this flammable gas are efficient storage and safe transport. The preferable way to solve the both problems is to choose solid porous materials as storage medium [1]. As a promising porous material, metal-organic frameworks (MOFs) have attracted more research interest in the field of hydrogen storage, owing to their high specific surface area, high volume, low density, and tunable pore size [2]. Recently, a large number of strategies have been developed to tune pore size and structure in MOFs for an optimal hydrogen uptake at low pressure [3,4]. Framework interpenetration, compared to non-interpenetrated form of the same framework, can further reduce the pore size and enhance the hydrogen uptake and thermal stability of MOFs, because smaller pores can result in higher H_2 heat of adsorption [4,5]. In view of the contribution of smaller pores to gas uptake, larger pores seemed to be detrimental for gas uptake at low pressure. But, more recently, Bai et al. investigated a batch of experiments on gas adsorption of nanoMOFs with high mesoporosity, which was attributed to a mass of mesopores including intercrystalline mesopores. They pointed out that nanoMOFs with the coexistence of micro- and mesopore possessed higher H_2 heat of adsorption for the strong physisorption from intercrystalline mesopores [6–8]. These results indicated that interpenetration and intercrystalline mesopores can be employed to optimize the gas uptake, respectively. Thus, the structure combining intercrystalline mesopores with interpenetration might possess high hydrogen uptake at low pressure. However, rare reports concern about the effect of introducing intercrystalline mesopores into the interpenetrated bulk MOFs on hydrogen adsorption.

MOF-5 is a representative MOFs because of its thermal stability and excellent hydrogen storage capacity [9,10]. Supramolecular templating method is one of the preparative methods for introducing intercrystalline meso-/macropores into materials [11]. Triethylamine (TEA), as organic amine, plays significant roles in formation of above-mentioned structures such as templating, deprotonating agent and charge-balancing agents [12].

In this paper, we synthesized an interpenetrated MOF-5 with high mesoporosity by adding TEA. The results showed that as-prepared materials can store 1.86 wt % hydrogen at 77 K under 1 atm, which was higher than the earlier reported hydrogen uptake of the interpenetrated MOF-5 with little mesopores under the same test condition. It is also implied that both intercrystalline mesopores and interpenetrated structure might result in enhancing hydrogen uptake of the as-prepared MOF-5 at low pressure.

2. Experimental

2.1. Materials

All chemicals were obtained commercially and used without further purification: zinc nitrate hexahydrate ($Zn(NO_3)_2 \cdot 6H_2O$) (XiLong Chemical Co., Ltd.), terephthalic acid (H_2BDC) (Sinopharm Chemical Reagent Co., Ltd.), N,N′-dimethylformamide (DMF) (XiLong Chemical Co., Ltd.), triethylamine (TEA) (XiLong Chemical Co., Ltd.), 4A-type molecular sieves (Sinopharm Chemical Reagent Co., Ltd.), and anhydrous chloroform (BeiJing Chemical Works).

* Corresponding author. Tel.: +86 10 82544091; fax: +86 10 82544096.
E-mail address: yurenwang@imech.ac.cn (Y. Wang).

0032-5910/$ – see front matter © 2013 Elsevier B.V. All rights reserved.
http://dx.doi.org/10.1016/j.powtec.2013.07.034

2.2. Methods

The procedure of synthesizing MOF-5 reported in the literature [13] was modified. The details are described as follows: The solvent DMF was first dehydrated for 24 h by 4A-type molecular sieves (activation at 400 °C for one day), and then $Zn(NO_3)_2 \cdot 6H_2O$ (1.664 g, 5.60 mmol) and H_2BDC (0.352 g, 2.12 mmol) were dissolved in 50 ml of dehydrated DMF solvent. TEA (550 μl) was added into the mixture and white precipitate was immediately removed. The transparent solution was quickly transferred to a 100 ml glass vial and sealed. The glass vial was then heated to 105 °C and held for 24 h. After the reaction, the vial was taken out of the oven and cooled down to room temperature naturally. The powders were collected from the solvent and washed thoroughly with DMF for three times. After that, the powders were immersed in 50 ml chloroform, sealed tightly at room temperature for 7 days. During the process, the chloroform solution was decanted and replenished every two days. The prepared MOF-5 powders were dried under vacuum at 155 °C for 24 h.

3. Characterization

Powder X-ray diffraction (XRD) pattern of sample was obtained on a Rigaku Ultima IV X-ray diffractometer with a Cu Kα1 radiation source (k = 1.54056 Å) operated at 40 kV and 40 mA at a scanning step of 0.01° in the 2θ range 5°–40°. The morphologies of sample were characterized using a HITACHI-S4300 Scanning electron microscope (SEM) and a PHILIPS CM 200 FEG transmission electron microscope. Fourier-transform infrared (FT-IR) spectra were recorded with an AVATAR 360 FT-IR spectrophotometer using a standard KBr pellet technique. Thermogravimetric analysis of the sample was carried out using TA TGA Q5000IR under N_2 stream with a heating rate of 5 °C/min from room temperature to 600 °C. The porosities and specific surface areas were measured with a Micromeritics ASAP 2020 gas sorption and porosimetry apparatus using nitrogen gas at 77 K. Before the measurements, the sample (0.1 g) was heated at 130 °C under vacuum for 10 h. The hydrogen adsorption capacity (volumetric method) was measured at 77 K under 1 atm pressure using the same gas sorption instrument. Before the hydrogen-uptake measurement, the sample (0.1 g) was heated at 130 °C under vacuum for 10 h.

4. Results and discussion

The powder X-ray diffraction studies (Fig. 1) can demonstrate that the samples with high crystallinity possess the structure of interpenetrated MOF-5. In typical synthesis methods, solvothermal is preferable for the growth of MOF-5 with high crystallinity. Sharpness and high intensity of the peaks indicate high crystallinity of the prepared bulk materials, which agrees with the SEM image of the prepared MOF-5. In addition, according to Fang et al., the ratio (denoted as R_2) of the intensity of the peak at 13.8° to that at 6.8° of the non-penetrated MOF-5 was low, while high R_2 implied an interpenetrated structure, especially when the ratio (denoted as R_1) of the intensity of the peak at 9.7° to that at 6.8° was low [14]. As shown in Fig. 1, the peaks of the samples have the same two-theta values as those of the reported MOF-5 materials. Moreover, it is worthwhile to note that the as-made MOF-5 possesses high R_2 and relative low R_1, and the relative XRD peak intensity of the prepared MOF-5 is similar to that of interpenetrated MOF-5 reported by Fang et al., except the peak at 8.4°. The presence of the peak at 8.4° might imply partial collapse of the interpenetrated structure in MOF-5 [10,15]. Furthermore, based on the study of Park et al., the reactant concentration might be the key factor to prepare interpenetrated MOF-5 [16]. Thus, the interpenetration frameworks are likely due to high reactant concentration. On the other hand, MOF-5 seed crystals can be easily detached or dissolved by a high concentration of organic acid. Therefore, as a deprotonating agent, TEA is used to prevent protons of organic acid from attacking the MOF crystals [13].

The FT-IR spectrum of the as-prepared MOF-5 is shown in Fig. 2. The samples exhibit a band at 3600 cm^{-1} and a broad band centered at 3460 cm^{-1} due to strongly bound water [17,18]. In the region between 3100 and 2850 cm^{-1}, several bands can be assigned to aromatic and aliphatic C–H stretching vibrations modes of benzene ring [18]. The bands at 1500 cm^{-1} and 1560 cm^{-1} are attributed to the asymmetric stretching of carboxylate group in the BDC, whereas the peak at 1380 cm^{-1} is due to the symmetric stretching of carboxylate group in BDC. In the region between 1300 and 700 cm^{-1}, several bands are observed that can be assigned to the out-of-plane vibrations of BDC [19]. The FT-IR spectrum of the samples indicates that there are no chemical changes in the as-prepared MOF-5.

In order to characterize the morphology and porous texture, the SEM and TEM images of the samples are given in Fig. 3. Fig. 3a shows each particle consists of the intergrown cubic crystals. According to the definition, interpenetration is that the frameworks are maximally displaced from each other by shifting the second framework exactly one half of the pore size in the 3D directions [1]. Thus, the unique morphology might be due to interpenetration. The SEM image with higher magnification is shown in Fig. 3b, it is clear to see meso- and macropores on the surface of the samples. Fig. 3c gives the disordered porous structure in the bulk MOF-5. Fig. 3d shows the intercrystalline mesopores in the interpenetrated MOF-5, which is similar to the observation of Bai et al. [6]. The meso/macroporous structure including intercrystalline mesopores in the resulting MOF-5 could be mostly attributed to the function of TEA template [20,21]. More detailed mechanisms are still under investigation.

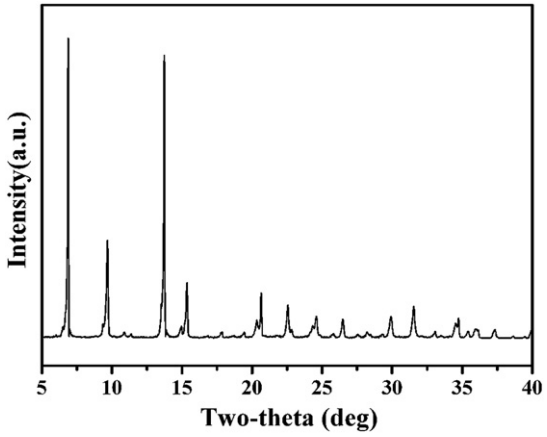

Fig. 1. XRD patterns of the as-prepared MOF-5.

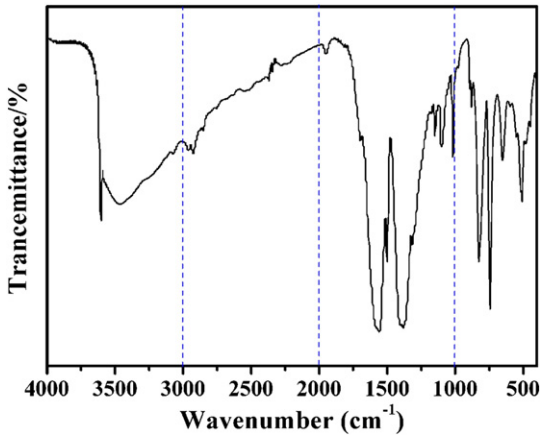

Fig. 2. FT-IR spectra of the as-prepared MOF-5.

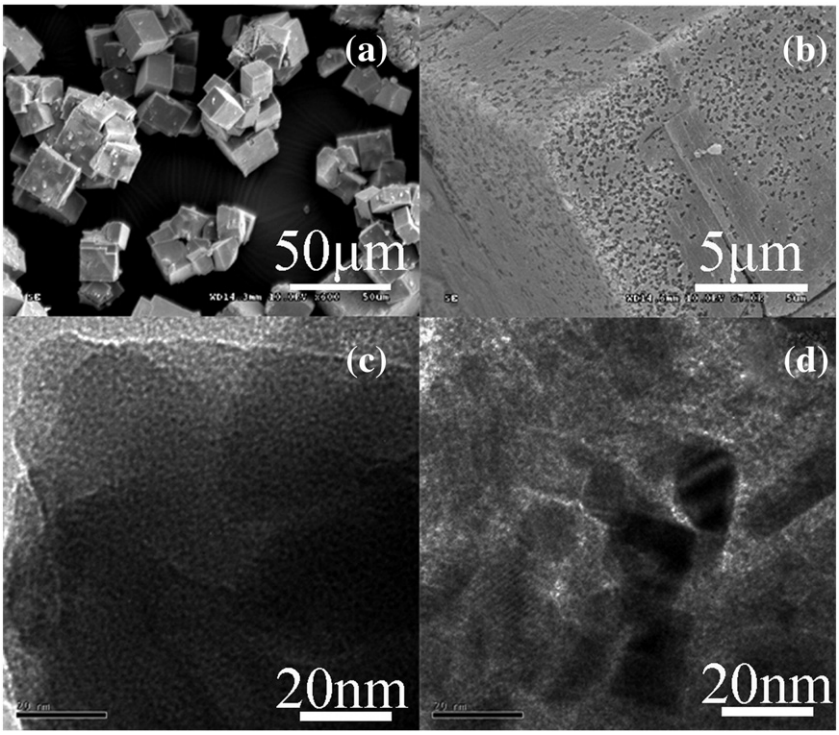

Fig. 3. SEM and TEM images of the as-prepared MOF-5. (a) SEM image, (b) SEM image with high magnification, (c) and (d) TEM images of pores in the samples.

The pore size and distribution of the samples can be further confirmed by the nitrogen adsorption and desorption analysis. The nitrogen adsorption and desorption isotherms of the samples are shown in Fig. 4a, and the inset shows a magnification of nitrogen adsorption/desorption isotherms in the relative pressure range 0.02–1.0. Pore size distributions are calculated by H–K method (Fig. 4b) and BJH method (Fig. 4c), respectively. Fig. 4a shows an initial steep increase in the volumetric uptake before 0.02 P/P_0 and then a quick saturation step at relative low pressure which signifies micropore filling, and a hysteresis loop at a relatively higher pressure, typically stemming

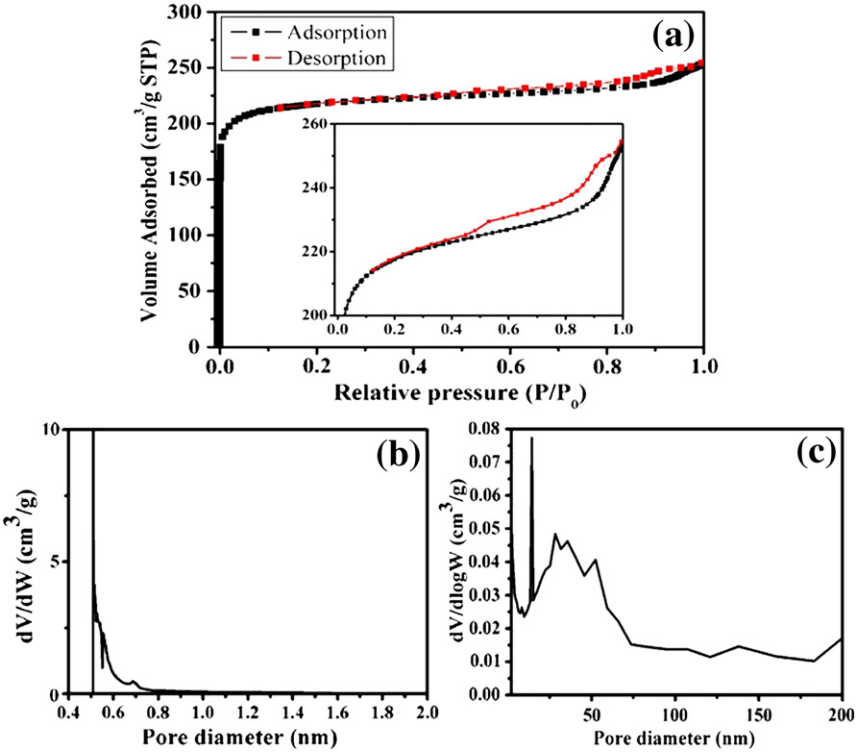

Fig. 4. (a) Nitrogen adsorption/desorption isotherms of the as-prepared MOF-5 at 77 K under 1 atm. Inset shows a magnification in 0.02–1.0 P/P_0. Pore size distribution of the samples calculated by (b) H–K method, (c) BJH method.

from the mesopores. Thus, nitrogen adsorption and desorption isotherms appear to have Type I character with H3 hysteresis loop (according to IUPAC classification) [22]. The results indicate that micro- and meso- even macropores coexist in the prepared MOF-5, which is consistent with the results of SEM and TEM. Fig. 4b shows that the micropores mainly distribute in the range of 0.52 nm–0.8 nm, which can suggest the interpenetrated structure in the prepared MOF-5. Because the micropore diameter of non-interpenetrated MOF-5 is commonly lager than 1 nm [23], the interpenetrated structure can decrease the pore size. And the mesoporous size distribution is in a wide range and the average mesopore diameter is about 6.2 nm using the BJH method (Fig. 4c). The pore volume contributed by the micropore in the interpenetrated MOF-5 is about 74%. And the BET specific surface area (SSA) of the interpenetrated MOF-5 with mesopore is only 732 m^2g^{-1}. As we know, the relatively low SSA of MOF-5 is mainly due to pore-filling, the interpenetrated structure [24], or the mesopores in the material [25]. The XRD and TGA curves can indicate that pore-filling is not the reason resulting in low SSA. Because XRD shows low intensity ratio of peak at 9.7° to that at 6.8° (low R_1) and might predict its pore without or with small amounts trapped zinc species or solvent [24]. In addition, the results of TGA further indicate no solvent and zinc species in the pores. As shown in Fig. 5, the initial weight loss below 100 °C is mainly due to desorption of water adsorbed on the surface. Then a rather sharp weight loss takes place after 375 °C and corresponds to the structural decomposition to ZnO. Except the two steps of weight loss, no distinct weight loss appears in 100–300 °C, and it means the activated temperature is efficient to remove the residual solvent in the pores. And zinc hydroxide, if trapped, will dehydrate at 125 °C [14]. Hence, the interpenetrated structure and the mesopore result in low SSA in this paper. Moreover, compared with the earlier reported MOF-5 [10], the temperature of thermal decomposition of the samples increases to 465 °C, owing to interpenetration resulting in high thermal stability.

Hydrogen isothermal adsorption and desorption curves of the interpenetrated MOF-5 with high mesoporosity are given in Fig. 6. The hydrogen adsorption capacity reaches 1.86 wt% at 77 K under 1 atm, which is greater than the reported interpenetrated MOF-5 without or with very small mesopores under the same testing condition [14,16]. In fact, large meso- and macropores in the as-prepared MOF-5 should be detrimental to hydrogen storage, because of no attraction from the surface of the pore walls to hydrogen molecules near the centre of the pore. But hydrogen uptake of the prepared MOF-5 can still reach to 1.86 wt%. The result suggests that intercrystalline mesopore plays an important role in hydrogen uptake of the interpenetrated MOF-5 at low pressure, which is likely due to the strong physisorption of hydrogen onto the unsaturated metal sites on the surface of intercrystalline

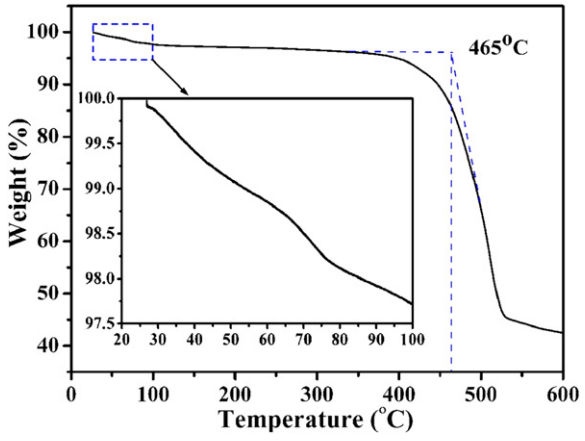

Fig. 5. Thermogravimetric curves of the as-prepared MOF-5. The inset shows a magnification of weight loss in the temperature range 25–100 °C.

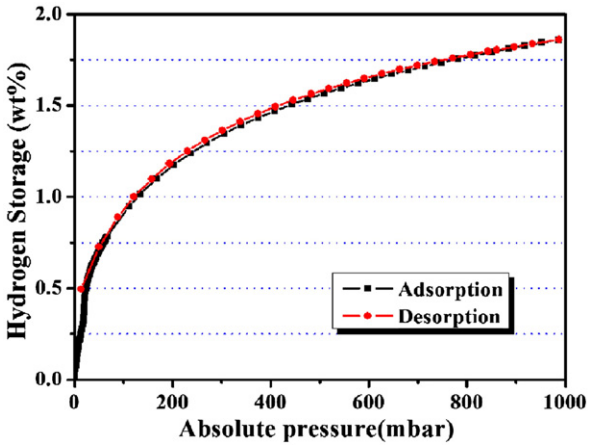

Fig. 6. Hydrogen adsorption/desorption isotherms of the as-prepared MOF-5 at 77 K under 1 atm.

mesopores [6]. On the other hand, interpenetration can efficiently improve the hydrogen uptake at low pressure. Thus, both intercrystalline mesopores and interpenetration can result in enhancing hydrogen uptake of the as-prepared MOF-5 at low pressure.

5. Conclusions

In summary, we prepared an interpenetrated MOF-5 with high mesoporosity via solvothermal synthesis and investigated its effects on the thermal stability and hydrogen uptake capacity. The results showed that the thermal decomposition temperature of this material was 465 °C, and hydrogen storage capacity reached 1.86 wt% at 77 K under 1 atm. The results suggested that the interpenetrated structure enhanced the thermal stability of the material, and both interpenetration and intercrystalline mesopores can enhance hydrogen storage of the as-prepared MOF-5 at low pressure. This study may have general implication for the other MOFs materials with improved thermal stability and enhanced hydrogen storage capacity at 77 K and low pressure.

Acknowledgements

The work wishes to acknowledge the National Natural Science Foundation of China (Nos. 11202211 and 11272315) and the support from the National Basic Research Program of China (973 Program, No. 2011CB710901).

References

[1] S.S. Han, J.L. Mendoza-Cortés, W.A. Goddard III, Recent advances on simulation and theory of hydrogen storage in metal-organic frameworks and covalent organic frameworks, Chem. Soc. Rev. 38 (2009) 1460–1476.
[2] K.L. Lim, H. Kazemian, Z. Yaakob, W.R.W. Daud, Solid-state materials and methods for hydrogen storage: a critical review, Chem. Eng. Technol. 33 (2010) 213–226.
[3] J.L.C. Rowsell, O.M. Yaghi, Strategies for hydrogen storage in metal-organic frameworks, Angew. Chem. Int. Ed. 44 (2005) 4670–4679.
[4] L.J. Murray, M. Dincă, J.R. Long, Hydrogen storage in metal-organic frameworks, Chem. Soc. Rev. 38 (2009) 1294–1314.
[5] T.B. Lee, D.H. Jung, D. Kim, J. Kim, K. Choi, S.H. Choi, Molecular dynamics simulation study on the hydrogen adsorption and diffusion in non-interpenetrating and interpenetrating IRMOFs, Catal. Today 146 (2009) 216–222.
[6] Z. Xin, J. Bai, Y. Pan, M.J. Zaworotko, Synthesis and enhanced H_2 adsorption properties of a mesoporous nanocrystal of MOF-5: controlling nano-/mesostructures of MOFs to improve their H_2 heat of adsorption, Chem. Eur. J. 16 (2010) 13049–13052.
[7] Z. Xin, J. Bai, Y. Shen, Y. Pan, Hierarchically micro- and mesoporous coordination polymer nanostructures with high adsorption performance, Cryst. Growth Des. 10 (2010) 2451–2454.
[8] H. Du, J. Bai, C. Zuo, Z. Xin, J. Hu, A hierarchical supra-nanostructure of HKUST-1 featuring enhanced H_2 adsorption enthalpy and higher mesoporosity, CrystEngComm 13 (2011) 3314–3316.
[9] H. Li, M. Eddaoudi, M. O'Keeffe, O.M. Yaghi, Design and synthesis of an exceptionally stable and highly porous metal-organic framework, Nature 402 (1999) 276–279.

[10] S.J. Yang, J.Y. Choi, H.K. Chae, J.H. Cho, K.S. Nahm, C.R. Park, Preparation and enhanced hydrostability and hydrogen storage capacity of CNT@MOF-5 hybrid composite, Chem. Mater. 21 (2009) 1893–1897.
[11] K. Egeblad, C.H. Christensen, M. Kustova, C.H. Christensen, Templating mesoporous zeolites, Chem. Mater. 20 (2008) 946–960.
[12] Q. Fang, G. Zhu, M. Xue, Z. Wang, J. Sun, S. Qiu, Amine-templated assembly of metal-organic frameworks with attractive topologies, Cryst. Growth Des. 8 (2008) 319–329.
[13] Y. Yoo, Z. Lai, H.K. Jeong, Fabrication of MOF-5 membranes using microwave-induced rapid seeding and solvothermal secondary growth, Microporous Mesoporous Mater. 123 (2009) 100–106.
[14] B. Chen, X. Wang, Q. Zhang, X. Xi, J. Cai, H. Qi, S. Shi, J. Wang, D. Yuan, M. Fang, Synthesis and characterization of the interpenetrated MOF-5, J. Mater. Chem. 20 (2010) 3758–3767.
[15] S.S. Kaye, A. Dailly, O.M. Yaghi, J.R. Long, Impact of preparation and handling on the hydrogen storage properties of Zn_4O(1,4-benzenedicarboxylate)$_3$ (MOF-5), J. Am. Chem. Soc. 129 (2007) 14176–14177.
[16] S.J. Yang, H. Jung, T. Kim, J.H. Im, C.R. Park, Effects of structural modifications on the hydrogen storage capacity of MOF-5, Int. J. Hydrogen Energy 37 (2012) 5777–5783.
[17] C. Petit, T.J. Bandosz, MOF-graphite oxide nanocomposites: surface characterization and evaluation as adsorbents of ammonia, J. Mater. Chem. 19 (2009) 6521–6528.
[18] S. Bordiga, J.G. Vitillo, G. Ricchiardi, L. Regli, D. Cocina, A. Zecchina, B. Arstad, M. Bjørgen, J. Hafizovic, K.P. Lillerud, Interaction of hydrogen with MOF-5, J. Phys. Chem. B 109 (2005) 18237–18242.
[19] M. Jahan, Q. Bao, J.X. Yang, K.P. Loh, Structure-directing role of graphene in the synthesis of metal-organic framework nanowire, J. Am. Chem. Soc. 132 (2010) 14487–14495.
[20] X. Ke, L. Xu, C. Zeng, L. Zhang, N. Xu, Synthesis of mesoporous TS-1 by hydrothermal and steam-assisted dry gel conversion techniques with the aid of triethanolamine, Microporous Mesoporous Mater. 106 (2007) 68–75.
[21] J. Zhou, Z. Hua, X. Cui, Z. Ye, F. Cui, J. Shi, Hierarchical mesoporous TS-1 zeolite: a highly active and extraordinarily stable catalyst for the selective oxidation of 2,3,6-trimethylphenol, Chem. Commun. 46 (2010) 4994–4996.
[22] K.S.W. Sing, D.H. Everett, R.A.W. Haul, L. Moscou, R.A. Pierotti, J. Rouquérol, T. Siemieniewska, Reporting physisorption data for gas/solid systems with special reference to the determination of surface area and porosity, Pure Appl. Chem. 57 (1985) 603–619.
[23] O.M. Yaghi, M. O'Keeffe, N.W. Ockwig, H.K. Chae, M. Eddaoudi, J. Kim, Reticular synthesis and the design of new materials, Nature 423 (2003) 705–714.
[24] J. Hafizovic, M. Bjørgen, U. Olsbye, P.D.C. Dietzel, S. Bordiga, C. Prestipino, C. Lamberti, K.P. Lillerud, The inconsistency in adsorption properties and powder XRD data of MOF-5 is rationalized by framework interpenetration and the presence of organic and inorganic species in the nanocavities, J. Am. Chem. Soc. 129 (2007) 3612–3620.
[25] C.S. Tsao, M.S. Yu, T.Y. Chung, H.C. Wu, C.Y. Wang, K.S. Chang, H.L. Chen, Characterization of pore structure in metal-organic framework by small-angle X-ray scattering, J. Am. Chem. Soc. 129 (2007) 15997–16004.